Available online at www.sciencedirect.com

ScienceDirect

IFAC PapersOnline CONFERENCE PAPER ARCHIVE

IFAC PapersOnLine 53-2 (2020) 16814–16819

Parameter Estimation for Dynamic Resource Allocation in Microorganisms: A Bi-level Optimization Problem ⋆

Francis Mairet * **Térence Bayen** **

* *Ifremer, Physiology and Biotechnology of Algae laboratory, rue de l'Ile d'Yeu, 44311 Nantes, France (e-mail: francis.mairet@ifremer.fr)*
** *Avignon Université, Laboratoire de Mathématiques d'Avignon (EA 2151) F-84018 France (e-mail: terence.bayen@univ-avignon.fr)*

Abstract: Given their key roles in almost all ecosystems and in several industries, understanding and predicting microorganism growth is of utmost importance. In compliance with evolutionary principles, coarse-grained or genome-scale models of microbial growth can be used to determine optimal resource allocation scheme under dynamic environmental conditions. Resource allocation approaches have given important qualitative results, but it still remains a gap towards quantitiative predictions. The first step in this direction is parameter calibration with experimental data. But fitting these models results in a bi-level optimization problem, whose numerical resolution involves complex optimization issues. As a case study, we present here a coarse-grained model describing how microalgae acclimate to a change in light intensity. We first determine using the Pontryagin maximum principle and numerical simulations the optimal strategy, corresponding to a turnpike with a chattering arc. Then, a bi-level optimization problem is proposed to calibrate the model with experimental data. To solve it, a classical parameter identification routine is used, calling at each iteration the `bocop` solver to solve the optimal control problem (by a direct method). The calibrated model is able to represent the photoacclimation dynamics of the microalga *Dunaliella tertiolecta* facing a down-shift of light intensity.

Keywords: Bi-level optimization, Optimal control, Pontryagin's principle, Chattering, Microbial growth, Microalgae

1. INTRODUCTION

Predicting microorganism growth is a key challenge, with huge implications for the comprehension of ecosystem dynamics and the development of bioprocesses. Optimization can be used to decipher microbial growth, assuming that microorganisms have acquired through evolution optimal strategies. This principle has allowed the development of very useful methods: Flux Balance Analysis (Orth et al., 2010), Resource Balance Analysis (Goelzer et al., 2011), etc. Under dynamic environmental conditions, the key idea is to represent microorganism growth as an optimal control problem of resource allocation, as proposed in Pavlov and Ehrenberg (2013). This can be done with coarse-grained models of microbial growth (Molenaar et al., 2009; Weiße et al., 2015). For example, in a previous work, we have determined using the Pontryagin maximum principle and numerical simulations the optimal strategy (involving a chattering arc (Borisov, 2000)) for a bacterial population facing a nutrient up-shift (Giordano et al., 2016; Yegorov et al., 2018), showing similarities with the mode of action of the alarmone ppGpp. Dynamic optimization of resource allocation can also be done with (genome-scale) metabolic networks (Waldherr et al., 2015; Reimers et al., 2017; Yang et al., 2019).

These approaches involve a number of (unknown) parameters, ranging from a few for coarse-grained models to hundreds, even thousands for genome-scale models. Literature or database can provide a first guess of parameter values, but model calibration with experimental data is a necessary step to go from qualitative results to quantitative predictions. To this end, model parameters can be determined numerically as the solution of a bi-level optimization problem, leading nonetheless to complex optimization issues.

As a proof of concept, our objective here is to calibrate a coarse-grained model which describes how microalgae acclimate to a change in light intensity. Actually, microalgae are known to reduce their chlorophyll content (and the associated proteins) under high light, when photons are in excess (MacIntyre et al., 2002). This mechanism - the so-called photoacclimation - plays an important and complex role in microalgal bioprocesses given the interplay between chlorophyll and light attenuation in dense cultures (Bernard et al., 2015; de Mooij et al., 2017). Additionally, considering photoacclimation is of utmost importance to better estimate carbon fixation by the phytoplankton in the ocean from remote measurements of chlorophyll

⋆ This research benefited from the support of the FMJH Program PGMO and from the support to this program from EDF-THALES-ORANGE.

10.1016/j.ifacol.2020.12.1163

(Graff et al., 2016). Optimality principles have already been used to tackle photoacclimation in static conditions (Armstrong, 2006; Zavřel et al., 2019) or for instantaneous growth rate maximization (Wirtz and Pahlow, 2010), but never to our knowledge over a time horizon.

After the presentation of the model (Section 2), we first determine the optimal allocation at steady-states (Section 3). Then, the optimal control problem is investigated using the Pontryagin maximum principle and numerical solutions obtained by the direct method using the `bocop` solver (Team Commands, Inria Saclay, 2017; Bonnans et al., 2017) (Section 4). We show that the optimal trajectory corresponds to a turnpike with a chattering arc. Finally, parameter estimation with experimental data is formulated as a bi-level optimization problem (Section 5). Parameters are estimated using a classical identification routine, calling at each iteration the `bocop` solver (Team Commands, Inria Saclay, 2017) to solve the optimal control problem. The calibrated optimal trajectory properly represents the dynamics of photoacclimation after a down-shift of light intensity.

2. MODEL DEVELOPMENT

We consider a coarse-grained model to represent photoacclimation in microalgae (see Fig. 1). Hereafter, c, p, and r represent respectively the proportion of carbon reserve (precursors), photosynthetic machinery (e.g., the light-harvesting complex LHCII), and gene expression machinery (e.g., ribosomal proteins). Cellular metabolism is represented by two macro-reactions: photosynthesis (precursor production) and protein synthesis, catalyzed respectively by the photosynthetic machinery and by the gene expression machinery. Using mass action kinetics, the photosynthetic rate and the protein synthesis rate are given respectively by:

$$v_P = \tilde{k}_P I p, \quad \text{and} \quad v_R = k_R c r$$

where I is the light intensity. For sake of simplicity, we will use in the following $k_P := \tilde{k}_P I$ given that a constant light intensity will be considered [1].

In the model, the variable $u \in [0;1]$ will represent the proportion of the protein synthesis flux allocated to the photosynthetic machinery. From mass balance, we get the following system:

$$\begin{aligned} \frac{dc}{dt} &= v_P - v_R - c v_P &&= k_P p - k_R c r - k_P p c, \\ \frac{dp}{dt} &= u v_R - p v_P &&= u k_R c r - k_P p^2, \\ \frac{dr}{dt} &= (1-u) v_R - r v_P &&= (1-u) k_R c r - k_P p r. \end{aligned} \tag{1}$$

Note that the last term in each equation corresponds to the effect of dilution by growth (see e.g., Giordano et al. (2016)). Finally, given that $c + p + r = 1$, we can reduce the dimension of the system:

$$\begin{cases} \dfrac{dc}{dt} = k_P p(1-c) - k_R c(1-c-p), \\ \dfrac{dp}{dt} = u(t) k_R c(1-c-p) - k_P p^2. \end{cases} \tag{2}$$

[1] The light intensity down-shift will occur at the initial time in the simulations.

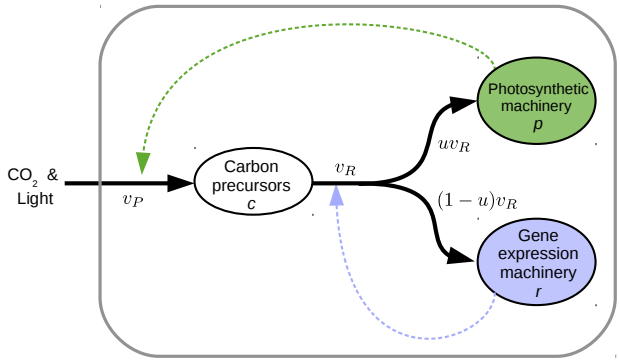

Fig. 1. Scheme of the coarse-grained model to represent photoacclimation in microalgae.

The system (2) satisfies the following invariance property.

Lemma 1. The set $\Omega := \{(c,p) \in (0,1)\times(0,1)\ ;\ c+p \leq 1\}$ is invariant by (2).

Proof. Whenever $c = 0$ (resp. $p = 0$), it is easily seen that $\dot{c} = k_P p > 0$ (resp. $\dot{p} = u(t) k_R c(1-c) > 0$), so the positive orthant is invariant. In addition, one has $\dot{c} + \dot{p} = 0$ along $c+p = 1$ so that the line segment $L := \{(c, 1-c)\ ; c \in [0,1]\}$ is also invariant. This ends the proof.

Since trajectories of (2) starting in L remain in L, we suppose next that initial conditions belong to the (open) invariant domain:

$$\mathcal{D} := \{(c,p) \in (0,1) \times (0,1)\ ;\ c + p < 1\}.$$

We assume that microalgae have acquired through evolution optimal strategy, i.e. they regulate their allocation of resources in order to maximize their growth. To represent this behavior, we are interested in maximizing the photosynthetic rate $v_P = k_P p$ w.r.t. the allocation of protein synthesis u (corresponding to our control) over a given time period. Thus, we consider the admissible control set defined as:

$$\mathcal{U} = \{u : [0,T] \to [0,1]\ ;\ \text{meas.}\},$$

in which $T > 0$ is our given time period. The optimization problem under consideration can be then gathered into:

$$\max_{u(\cdot)\in\mathcal{U}} J(u) := \int_0^T k_P p(t)\, \mathrm{d}t, \tag{P}$$

where $(c(\cdot), p(\cdot))$ is the unique solution of (2) starting at a given point $(c_0, p_0) \in \mathcal{D}$ for a given control $u \in \mathcal{U}$.

3. STATIC OPTIMIZATION PROBLEM

Before investigating further optimal controls, it is interesting to study the static optimization problem:

$$\max_{u\in[0,1]} \bar{J}(u) := k_P p_u, \tag{3}$$

where (c_u, p_u) is a steady state of (2) associated with the constant control u, i.e.,

$$\begin{aligned} 0 &= k_P p_u (1-c_u) - k_R c_u (1-c_u-p_u), \\ 0 &= u k_R c_u (1-c_u-p_u) - k_P p_u^2. \end{aligned}$$

Indeed, we shall see that solutions of the dynamic optimization problem (P) are related to solutions of the static problem (3). In the sequel, we set $\omega := \frac{k_P}{k_R} > 0$.

Lemma 2. Problem (3) admits a unique optimal solution $(u^\star, c^\star, p^\star)$ given by

$$(u^\star, c^\star, p^\star) = \left(\frac{1}{1+\sqrt{\omega}}, \frac{\sqrt{\omega}}{1+\sqrt{\omega}}, \frac{1}{(1+\sqrt{\omega})^2}\right). \quad (4)$$

Proof. Combining the two equations at steady state implies that $p_u = u(1-c_u)$. Replacing p_u by its value into the first equation then gives

$$c_u = \frac{\omega u}{\omega u + 1 - u}.$$

Since we want to maximize the function $u \mapsto u(1-c_u)$ over $[0,1]$, we thus obtain that u is a solution to the equation $(1-\omega)x^2 - 2x + 1 = 0$ which gives us the unique solution (in $[0,1]$) $u^\star := \frac{1}{1+\sqrt{\omega}} \in [0,1]$. The value of $(c^\star, p^\star)$ follows.

Recalling that $\omega = k_P/k_R = I\tilde{k}_P/k_R$, we obtain that the optimal photosynthetic machinery sector at equilibrium $p^\star$ is a decreasing function of light intensity I, in line with experimental data of steady-state photoacclimation (MacIntyre et al., 2002), see Fig. 2. Actually, this pattern has already been predicted by steady-state optimization with similar models (e.g. in Armstrong (2006)).

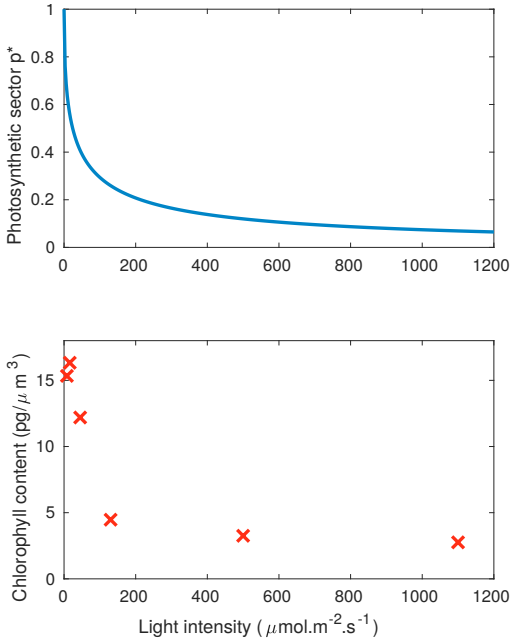

Fig. 2. Optimal steady-state allocation for the photosynthetic sector $p^\star$ as a function of light intensity (top), see Lemma 2. This pattern corresponds to the photoacclimation phenomena (MacIntyre et al., 2002), as shown for example by the chlorophyll content measured experimentally for *Dunaliella tertiolecta* (Havelková-Doušová et al., 2004) (bottom).

We have the following stability property near the optimal steady-state.

Proposition 3. The steady-state $(c^\star, p^\star)$ of (2) associated with the (constant) control $u = u^\star$ is locally stable with two negative eigenvalues.

Proof. The Jacobian matrix of (2) for $u = u^\star$ at $(c^\star, p^\star)$ is given by

$$\begin{bmatrix} a & b \\ c & d \end{bmatrix}$$

with $a := 0$, $b := \frac{\omega+\sqrt{\omega}}{1+\sqrt{\omega}}$, $c := -\frac{\omega}{(1+\sqrt{\omega})^3}$, $d := -\frac{\omega(1+4\sqrt{\omega}+2\omega)}{(1+\sqrt{\omega})^4}$. A computation of trace and determinant of A then gives $\mathrm{Tr}(A) = d < 0$ and $\det(A) = \frac{\omega(\omega+\sqrt{\omega})}{(1+\sqrt{\omega})^4} > 0$ which ends the proof.

4. COMPUTATION OF AN OPTIMAL CONTROL

4.1 Pontryagin's Principle

The optimization problem (P) is an optimal control problem. Optimal controls can be derived using the Pontryagin Maximum Principle (see Pontryagin et al. (1964)). Note that the existence of an optimal control is straightforward (due to the linearity of (2) w.r.t. the control), this follows from Fillipov's Theorem (Cesari, 2012). Let us now turn to Pontryagin's Principle. Doing so, let $H = H(c, p, \lambda_c, \lambda_p, \lambda^0, u)$ be the Hamiltonian associated with (P):

$$H := k_R c(1-c-p)\left[u\lambda_p - \lambda_c\right] + k_P p\left[\lambda_c(1-c) - \lambda_p p - \lambda^0\right].$$

Let u be an optimal control and let $x(\cdot) = (c(\cdot), p(\cdot))$ be the associated trajectory. Then, there exists $\lambda^0 \leq 0$ and an absolutely continuous map $\lambda = (\lambda_c, \lambda_p) : [0,T] \to \mathbb{R}^2$ such that $(\lambda, \lambda^0) \neq 0$ and $\dot{\lambda} = -\frac{\partial H}{\partial x}$, that is:

$$\dot{\lambda}_c = -k_R(1-2c-p)(u\lambda_p - \lambda_c) + k_P p\lambda_c, \quad (5)$$

$$\dot{\lambda}_p = k_R c(u\lambda_p - \lambda_c) - k_P\left[\lambda_c(1-c) - 2\lambda_p p - \lambda^0\right]. \quad (6)$$

In addition, transversality conditions imply $\lambda_c(T) = \lambda_p(T) = 0$ since the terminal state is free. It follows that $\lambda^0 < 0$, i.e., no abnormal trajectories occur (otherwise, we would have $\lambda_c \equiv 0$ and $\lambda_p \equiv 0$ implying that the pair (λ, λ^0) would be zero and a contradiction). By homogeneity of the Hamiltonian, we may assume that $\lambda^0 = -1$. The Hamiltonian condition in Pontryagin's Principle then gives

$$u(t) \in \mathrm{argmax}_{v\in[0,1]} H(x(t), \lambda(t), -1, v) \quad \text{a.e. } t \in [0,T]. \quad (7)$$

An extremal is a triplet $(x(\cdot), \lambda(\cdot), u(\cdot))$ satisfying (2)-(5)-(7) (since $\lambda^0 < 0$, we thus only consider normal extremals in the sequel). From (7), the control law is given by the sign of the *switching function*

$$\phi := \lambda_p k_R c(1-c-p),$$

which gives

$$\begin{cases} \phi(t) > 0 \;\Rightarrow\; u(t) = 1, \\ \phi(t) < 0 \;\Rightarrow\; u(t) = 0. \end{cases}$$

Of particular interest is the case where ϕ vanishes over a sub-interval $[t_1, t_2] \subset [0,T]$. In that case, we say that the extremal is singular over $[t_1, t_2]$ and that a singular arc occurs. We will now study whether or not this phenomenon takes place.

4.2 Study of singular arcs

In this section, we suppose that an extremal trajectory is singular over a time interval $[t_1, t_2]$, and we compute singular controls. In particular, it gives us a relationship between the solution to the static optimization problem and singular arcs.

Proposition 4. Along a singular arc, one has :

$$\begin{cases} u(t) = u^\star, \\ c(t) = c^\star, \\ p(t) = p^\star. \end{cases} \tag{8}$$

Proof. Let then $I := [t_1, t_2] \subset [0, T]$ be such that $\phi(t) = \dot{\phi}(t) = 0$, for every $t \in [t_1, t_2]$. Because initial conditions are in $\mathcal{D}$, this amounts to have $\lambda_p(t) = 0$ and $\dot{\lambda}_p(t) = 0$ for every $t \in I$. From $\dot{\lambda}_P(t) = 0$, we thus find

$$\lambda_C = -\frac{\omega}{c + \omega(1-c)}.$$

We then have $\ddot{\lambda}_P(t) = 0$ for every $t \in I$, hence, using that $\lambda_p(t) = \dot{\lambda}_p(t) = 0$ for $t \in [t_1, t_2]$, we find that

$$\lambda_c \dot{c}(\omega - 1) - \dot{\lambda}_c(c + \omega(1-c)) = 0,$$

that is,

$$\begin{aligned}(\omega p(1-c) - c(1-c-p))(\omega - 1) \\ - (c + \omega(1-c))(p\omega + 1 - 2c - p) = 0.\end{aligned}$$

Solving this equation w.r.t. c gives

$$c = c^\star \quad \text{or} \quad c = \tilde{c} := \frac{-\sqrt{\omega}}{1 - \sqrt{\omega}} < 0,$$

hence we conclude that $c = c^\star$ is constant over $[t_1, t_2]$. It follows that λ_C is constant. Hence $\dot{\lambda}_C = 0$, but, since $\dot{\lambda}_c = \lambda_c(pk_P + k_R(1-2c-p))$, it follows that $pk_P + k_R(1-2c-p) = 0$. Hence, $p = \frac{1}{(\sqrt{\omega}+1)^2} = p^\star$. We have thus shown that the singular arc corresponds to the optimal steady-state. The value of the singular control immediately follows from the state equation, and we find that $u(t) = u^\star$ for $t \in [t_1, t_2]$.

Using the previous computations, it can be observed that the control u does not appear in the second derivative of the switching function $\ddot{\phi}$, hence, we can conclude that the singular arc is at least of order $q \geq 2$. We conjecture that the singular arc is of second order, so an optimal trajectory can enter into the singular arc only by a *chattering arc* (which contains an infinite number of switching points) (Marchal, 1973; Borisov, 2000), as in the well-known Fuller's Problem. Rigorously, one should check that the Kelley necessary optimality condition

$$(-1)^q \frac{\partial}{\partial u} \frac{d^{2q}}{dt^{2q}} \phi(t) < 0, \quad t \in [t_1, t_2],$$

is fulfilled along the singular arc (note that if such a condition is violated, then no singular arc occurs). Even with small models, this computation becomes laborious. Therefore, our conjecture will be confirmed in the next section thanks to numerical simulations by a direct method.

4.3 Optimal trajectories

In line with the Maximum Principle and the Kelley condition, we conjecture that optimal solutions consist in a transient towards the optimal steady-state, and then to stay on this point (turnpike). The transient should be a chattering arc (i.e. with an infinite number of switching between $u = 0$ and $u = 1$).

Finally, we solve numerically the optimal control problem by the direct method using the software `bocop` (Team Commands, Inria Saclay, 2017; Bonnans et al., 2017). A time discretization allows to transform the optimal control problem into a nonlinear optimization problem, solved here by interior point techniques. A discretization by a Lobatto IIIC formula (6th order) was used with 400 time steps, and the relative tolerance for NLP solver was set at 10^{-10}. The optimal trajectories obtained numerically are composed of a chattering arc followed by a constant singular arc (which corresponds to the optimal steady state), see Fig. 3. Then, a second chattering arc escaping from the singular arc appears at the end of the simulation. For our biological problem, this arc corresponds to an artifact due to a fixed final time, and only the transition from the initial condition to the optimal steady-state is relevant.

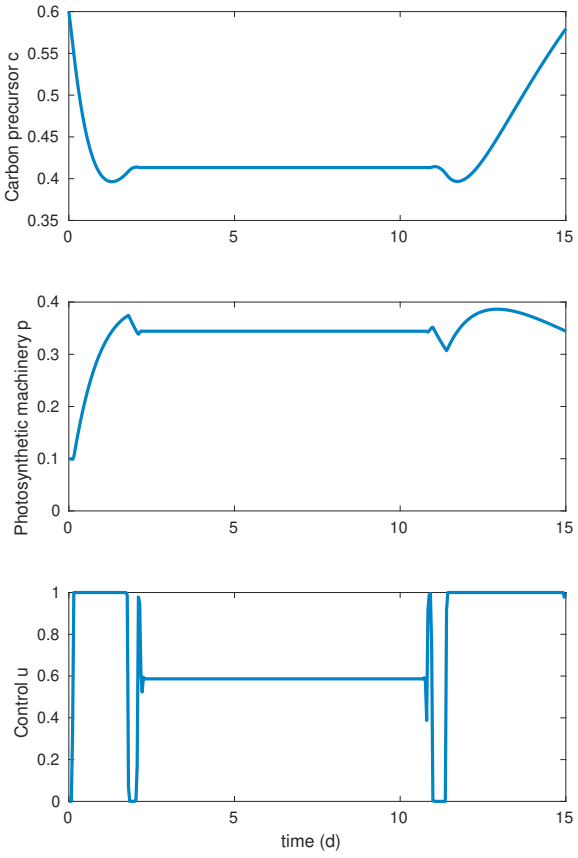

Fig. 3. Optimal trajectory (solution of (P)), obtained numerically by the direct method using the `bocop` solver (Team Commands, Inria Saclay, 2017). It is composed of a chattering arc (from t=0 to 2 d), a constant singular arc corresponding to the optimal steady state (from t=2 to 11 d), and finally a second chattering arc escaping from the singular arc.

These numerical results tend to confirm our conjecture: the optimal strategy is a turnpike with chattering. Additionally, these results show the reliability of the numerical method. Trajectories are actually computed by the direct method, without any knowledge of the theoretical solution, and the numerical solutions presents several characteristics demonstrated previously (the singular arc corresponds to the optimal steady states, and the trajectories join this arc with a chattering arc).

5. PARAMETER ESTIMATION

We want to evaluate if this framework allows to represent quantitatively microorganism growth, so the model parameters θ should be estimated with experimental data. The model output is given by:

$$y(t) = g(x(t), \theta).$$

We consider a set of measurements $\bar{y}_k \in \mathbb{R}^m$, corresponding to time instants $t_1, \dots, t_{n_k}$, $k \geq 1$. Our objective is to find the set of parameters $\theta = (k_P, k_R)^T$ such that the optimal solution $x(\cdot)$ of (P) fits the experimental data. This leads to a so-called *bi-level optimization problem*:

$$\min_{\theta \in C} \sum_k \left(g(x^*(t_k), \theta) - \bar{y}_k\right)^T Q \left(g(x^*(t_k), \theta) - \bar{y}_k\right)$$

$$\text{s.t.} \left| \begin{array}{ll} u^* & \in \text{argmax}_{u \in \mathcal{U}} \displaystyle\int_0^T k_P p(t)\, \mathrm{d}t, \\ \dot{x}(t) & = f(x(t), u(t), \theta) \quad \text{a.e. } t \in [0, T], \\ x(0) & = x_0, \end{array} \right. \tag{9}$$

where Q is a weighting matrix, C is a non-empty compact subset of $\mathbb{R}^2$, $f(\cdot, \cdot, \cdot)$ is the dynamics given by System (2) (in which we incorporate the dependency w.r.t. the two parameters), and x^* is the solution to this system associated with u^*. Problem (P) plays the role of *lower level program* whereas the optimization w.r.t. θ in (9) is the *upper level program*. Problem (9) is unusual because it couples an optimal control problem to a non-linear program.

Experimental data with the microalga *Dunaliella tertiolecta* (Sukenik et al., 1990) have been considered. After several days of acclimation at 700 μmol.m^{-2}.s^{-1}, light intensity has been shifted down to 70 μmol.m^{-2}.s^{-1} at $t = 0$. The following measurements have been used for parameter estimation:

- The relative content of LHCII, determined from Western blots. We consider that the photosynthetic sector p follows the same relative dynamics as this protein, and we fix arbitrarily the initial condition $p(0) = 0.1$.
- The photosynthetic rate (v_P), given in mole C.cell^{-1}.s^{-1} and converted in d^{-1} assuming a carbon content of 3.5 pmole C.cell^{-1} (determined by equilibrium values at low light).
- The specific growth rate, which we assume correspond to $v_R/(p + r)$, i.e. the protein synthesis rate per unit of protein.

The solution of the bi-level optimization problem (9) is determined using a classical direct search routine (by the Nelder-Mead method in Python). At each iteration, the `bocop` solver is called to solve the lower level problem for a given θ. We take 400 time steps, with a time horizon large enough such that the second chattering arc occurs after the last measurement (this final arc is not relevant in our biological problem). For each variable, the square errors between the measurements and the optimal trajectory are weighted by the inverse of the square of the measurement mean. The computation time to solve the bi-level optimization problem on a classical laptop was six minutes. The estimated parameters k_P and k_R are given in Table 1, and the associated optimal trajectory is shown on Fig. 4, with also the experimental data used in (9).

Table 1. Parameters estimated as the solution of the bi-level optimization problem (9)

Parameter		Value	Unit
Photosynthetic rate constant	k_P	1.01	d^{-1}
Protein synthesis rate constant	k_R	2.03	d^{-1}

Although our coarse-grained model involves many assumptions, the simulation properly represents the dynamics of photoacclimation. This is the first hint that our approach is effective, and it should now be validated with other experiments. The optimal control - involving a chattering arc - is biologically inconceivable. Nonetheless, the simulated trajectory fits well the data. Actually, Giordano et al. (2016) have shown that a simple (and biologically plausible) controller can give trajectories and performances very similar to the optimal ones. We thus expect that the state dynamics are coherent, even if the control is not realistic. To obtain smoother trajectories, a cost on the control can actually be considered (Cinquemani et al., 2019), or the number of time steps can be decreased (which additionally will also reduce computation time).

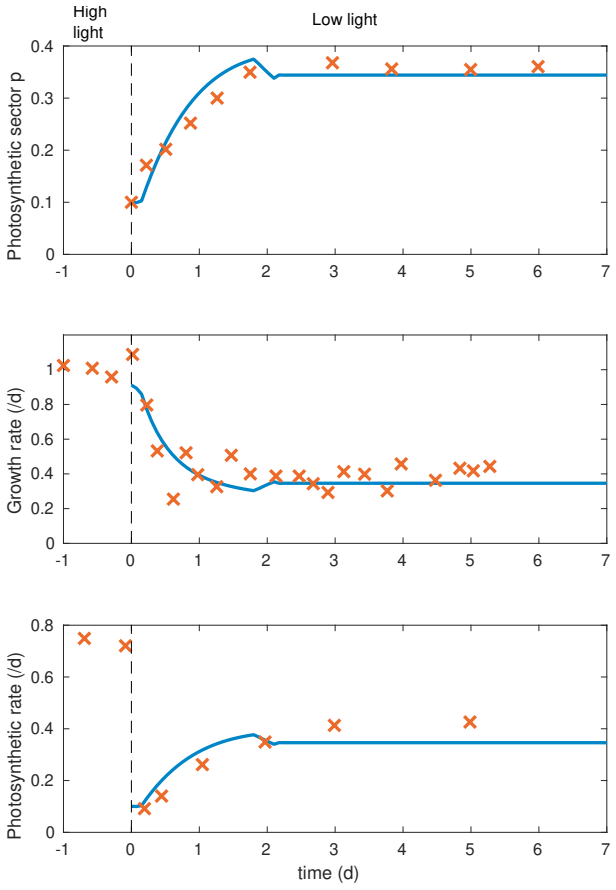

Fig. 4. Trajectory corresponding to the solution of the bi-level optimization problem (9). The model (blue lines) fits the experimental data (red crosses) of the microalga *Dunaliella tertiolecta* facing a light intensity down-shift from 700 μmol.m^{-2}.s^{-1} to 70 μmol.m^{-2}.s^{-1} at $t = 0$ (Sukenik et al., 1990).

6. CONCLUSION

A coarse-grained model of microalgal photoacclimation has been proposed as a case study for quantitative prediction of microbial growth in dynamic conditions. The optimal allocation strategy was first determined using the Pontryagin maximum principle and numerical solutions obtained by the direct method using the `bocop` solver. We have shown that the optimal trajectory corresponds to a turnpike with a chattering arc. Then, model parameters have been computed as solutions to a bi-level optimization problem. The calibrated optimal trajectory properly represents the dynamics of photoacclimation after a downshift of light intensity. This shows that our framework can be used for quantitative estimation of microbial growth and resource allocation in dynamic conditions.

When dealing with genome-scale models (*i.e.*, when increasing the numbers of states, controls, and parameters), the aforementioned fitting procedure will surely become too heavy. As a future work, we aim to find optimality conditions for such a bi-level problem and to develop more efficient numerical tools to perform parameter uncertainty analysis and to tackle more complex models.

ACKNOWLEDGEMENTS

The authors are grateful to Pierre Martinon (Inria) for providing support on the software `bocop`.

REFERENCES

Armstrong, R. (2006). Optimality-based modeling of nitrogen allocation and photoacclimation in photosynthesis. *Deep Sea Research Part II: Topical Studies in Oceanography*, 53(5-7), 513–531.

Bernard, O., Mairet, F., and Chachuat, B. (2015). Modelling of microalgae culture systems with applications to control and optimization. In *Microalgae Biotechnology*, 59–87. Springer.

Bonnans, Frederic, J., Giorgi, D., Grelard, V., Heymann, B., Maindrault, S., Martinon, P., Tissot, O., and Liu, J. (2017). Bocop A collection of examples. Technical report, INRIA. URL `http://www.bocop.org`.

Borisov, V. (2000). Fuller's phenomenon: Review. *Journal of Mathematical Sciences*, 100(4), 2311–2354.

Cesari, L. (2012). *Optimizationtheory and applications: problems with ordinary differential equations*, volume 17. Springer Science & Business Media.

Cinquemani, E., Mairet, F., Yegorov, I., de Jong, H., and Gouzé, J.L. (2019). Optimal control of bacterial growth for metabolite production: The role of timing and costs of control. In *2019 18th European Control Conference (ECC)*, 2657–2662. IEEE.

de Mooij, T., Nejad, Z.R., van Buren, L., Wijffels, R.H., and Janssen, M. (2017). Effect of photoacclimation on microalgae mass culture productivity. *Algal research*, 22, 56–67.

Giordano, N., Mairet, F., Gouzé, J.L., Geiselmann, J., and de Jong, H. (2016). Dynamical allocation of cellular resources as an optimal control problem: Novel insights into microbial growth strategies. *PLOS Computational Biology*, 12(3), e1004802.

Goelzer, A., Fromion, V., and Scorletti, G. (2011). Cell design in bacteria as a convex optimization problem. *Automatica*, 47(6), 1210–1218.

Graff, J.R., Westberry, T.K., Milligan, A.J., Brown, M.B., Olmo, G.D., Reifel, K.M., and Behrenfeld, M.J. (2016). Photoacclimation of natural phytoplankton communities. *Marine Ecology Progress Series*, 542, 51–62.

Havelková-Doušová, H., Prášil, O., and Behrenfeld, M. (2004). Photoacclimation of *Dunaliella tertiolecta* (chlorophyceae) under fluctuating irradiance. *Photosynthetica*, 42(2), 273–281.

MacIntyre, H., Kana, T., Anning, T., and Geider, R. (2002). Photoacclimation of photosynthesis irradiance response curves and photosynthetic pigments in microalgae and cyanobacteria. *J.Phycol.*, 38(1), 17–38.

Marchal, C. (1973). Chattering arcs and chattering controls. *J. Optimiz. Theory App.*, 11(5), 441–468.

Molenaar, D., Van Berlo, R., De Ridder, D., and Teusink, B. (2009). Shifts in growth strategies reflect tradeoffs in cellular economics. *Mol. Syst. Biol.*, 5(1), 323.

Orth, J.D., Thiele, I., and Palsson, B.Ø. (2010). What is flux balance analysis? *Nature biotechnology*, 28(3), 245.

Pavlov, M.Y. and Ehrenberg, M. (2013). Optimal control of gene expression for fast proteome adaptation to environmental change. *Proceedings of the National Academy of Sciences*, 110(51), 20527–20532.

Pontryagin, L., Boltyanskiy, V., Gamkrelidze, R., and Mishchenko, E. (1964). *Mathematical theory of optimal processes*. New York.

Reimers, A.M., Knoop, H., Bockmayr, A., and Steuer, R. (2017). Cellular trade-offs and optimal resource allocation during cyanobacterial diurnal growth. *PNAS*, 114(31), E6457–E6465.

Sukenik, A., Bennett, J., Mortain-Bertrand, A., and Falkowski, P.G. (1990). Adaptation of the photosynthetic apparatus to irradiance in *Dunaliella tertiolecta*: a kinetic study. *Plant physiology*, 92(4), 891–898.

Team Commands, Inria Saclay (2017). Bocop: an open source toolbox for optimal control. http://bocop.org.

Waldherr, S., Oyarzún, D.A., and Bockmayr, A. (2015). Dynamic optimization of metabolic networks coupled with gene expression. *Journal of theoretical biology*, 365, 469–485.

Weiße, A.Y., Oyarzún, D.A., Danos, V., and Swain, P.S. (2015). Mechanistic links between cellular trade-offs, gene expression, and growth. *Proceedings of the National Academy of Sciences*, 112(9), E1038–E1047.

Wirtz, K.W. and Pahlow, M. (2010). Dynamic chlorophyll and nitrogen: carbon regulation in algae optimizes instantaneous growth rate. *Marine Ecology Progress Series*, 402, 81–96.

Yang, L., Ebrahim, A., Lloyd, C.J., Saunders, M.A., and Palsson, B.O. (2019). DynamicME: dynamic simulation and refinement of integrated models of metabolism and protein expression. *BMC systems biology*, 13(1), 2.

Yegorov, I., Mairet, F., and Gouzé, J.L. (2018). Optimal feedback strategies for bacterial growth with degradation, recycling, and effect of temperature. *Optimal Control Applications and Methods*, 39(2), 1084–1109.

Zavřel, T., Faizi, M., Loureiro, C., Poschmann, G., Stühler, K., Sinetova, M., Zorina, A., Steuer, R., and Červenỳ, J. (2019). Quantitative insights into the cyanobacterial cell economy. *eLife*, 8, e42508.